

Canine Corneal Stromal Cells have multipotent mesenchymal stromal cell properties *in vitro*

Christiane Kafarnik^{1,2}, Alyce McClellan¹, Marc Dziasko², Julie T. Daniels², Deborah J. Guest¹

1 Centre for Preventive Medicine, Animal Health Trust, Newmarket, UK;

2 Rescue, Repair & Regeneration Theme, Institute of Ophthalmology, University College London, UK

Running head of title: Corneal stromal stem cells in dogs

Corresponding author: Christiane Kafarnik, Dr.med.vet., DipECVO; Centre for Preventive Medicine, Animal Health Trust, Lanwades Park, Newmarket, CB87UU, UK

Telephone: +44-1638 751000, Fax: +44 -1638 555391

Email: chka@arcor.de

Funding: Petplan Charitable Trust S16-204-397; European College of Veterinary Ophthalmologists research grant 2017

Key words: canine, dog, cornea, mesenchymal stromal cell, stem cells, corneal stromal stem cells

Abstract

The objective of this study was to determine whether corneal stromal cells (CSC) from the limbal and central corneal stroma in dogs have multipotent mesenchymal stromal cell (MSC) properties, and whether this cell population can be differentiated into keratocyte-like cells (KDC). Normal, donated, mesocephalic dog corneas were used to isolate CSC *in vitro*. Immunohistochemistry (IHC) demonstrated a distinct population of CD90 expressing cells in the anterior stroma throughout the limbal and central cornea. CSC could be cultured from both the limbal and central cornea and the culture kinetics showed a progenitor cell profile. The CSC expressed stem cell markers CD90, CD73, CD105, N-cadherin and Pax6 whereas CD34 was negative. Limbal and central CSC differentiated into osteoblasts, chondrocytes and adipocytes confirming their multipotency. Co-culturing allogeneic peripheral blood mononuclear cells (PBMCs) with limbal CSCs did not affect baseline PBMC proliferation indicating a degree of innate immune privilege. Limbal CSC could be differentiated into KDCs that expressed Keratocan, Lumican and ALDH1A3, and downregulated Pax6 and N-cadherin. In conclusion canine corneal stromal cells have multipotent MSC properties similarly described in humans and could serve as a source of cells for cell therapy and studying corneal diseases.

Introduction

The cornea is an optically clear tissue permitting light transmission into the eye and is essential for the biodefense and refractive system of the eye [1]. The basic anatomical structure of the cornea between mammals is similar. It is composed of an anterior epithelium and its basement membrane, the stroma, the Descemet's membrane, which is the basement membrane formed by the single layered posterior endothelium. However, a distinct layer comparable to the anterior limiting lamina (Bowman's layer) that is present in the human cornea does not exist in dogs [2,3].

Dogs can suffer from inherited diseases affecting the cornea, such as corneal crystalline dystrophy and corneal fibrosis which remains one of the leading causes of blindness in animals and people worldwide [4,5]. Blindness has severe consequences for working dogs but also negatively affects the quality of life in pet dogs. In contrast to human ophthalmology, corneal transplantation is rarely performed in dogs. This is due to a shortage of donors, expensive storage costs, and the lack of a canine corneal tissue bank [6].

Funderburgh et al. (2005) described a population of Pax6 expressing cells (<4%) in the bovine corneal stroma and identified them as progenitor cells. Stromal cells expressing mesenchymal stem cell (MSC) markers in the anterior stroma close to the limbus and central cornea, were also identified in humans [7]. A recent publication has also described a stromal stem cell population that originates from the human central corneal stroma [8]. Corneal stromal cells of the limbus in humans were found to fulfill the minimal criteria of The International Society for Cellular Therapy (ISCT) for multipotent MSCs [9-11]. *In vitro*, human corneal stromal cells also referred to as corneal stromal stem cells (CSSC) were differentiated into keratocytes that expressed Lumican, Keratocan, and ALDH1A1 and lost expression of Pax6 and ABCG2 [12-14]. A stable keratocyte phenotype has been described in relation to the differentiation process [15].

Similar to many other multipotent MSCs, CSSC are described to have immunomodulatory properties, which has relevance for preventing graft rejection for the purpose of tissue engineering. An *in vivo* study in mice has shown lack of tissue rejection after injecting CSSC

in a corneal fibrosis model [16]. A study using a mixed lymphocyte reaction with limbal CSSC showed an inhibition of the proliferation of activated PBMCs [8].

To date, CSSCs are thought to primarily have a support function for limbal epithelial stem cells (LESC). This is reinforced by the fact that basal epithelial cells in the limbal niche are in direct contact with stromal cells, both cells produce N-cadherin, a cell-cell junction protein and LESC co-cultured with CSSC have higher expansion and clonogenicity rates [17,18]. However, they may also have a role in corneal tissue homeostasis as an *ex vivo* model culturing sheep corneas with seeded CSSC after a LASIK procedure (laser in situ keratomileusis) showed significantly increased adherence of LASIK-like flaps while maintaining corneal transparency [8,19].

The current literature is based mainly on human, murine, rabbit and porcine corneal cells [20,21] but studies in canine corneas are not available. This led to the aim of the study to locate and characterize corneal stromal cells in dogs and investigate whether they have multipotent MSC properties. This study will provide a baseline for researchers working with canine corneal disease models and for potential cell-based therapy in veterinary ophthalmology.

Materials and Methods Donor material, selection and exclusion criteria

Corneas were isolated from 14 healthy donor corneas of dogs euthanized for reasons unrelated to this project and with the consent of the Animal Health Trust Ethical Review Committee (AHT_31_2013). Before excision of the corneal scleral buttons, the eyes were examined using a handheld slit lamp (KOWA SL14, Kowa Company LTD, Naka-ku, Nagoya, Aichi, Japan) by a board-certified veterinary ophthalmologist (CK).

The mean ages (\pm SD, range) of corneal donors was 4.61 years (\pm 3.97; median: 2; range: 0.2-12 years). There were eight different mesocephalic breeds included, brachycephalic breeds were excluded. The gender distribution was composed of intact males (n= 6), intact female (n= 1), spayed females (n= 4) and neutered males (n= 3). Details about the donor tissues are listed in the Supplementary table 1.

Cultured CSCs of each donor were expanded, cryopreserved and then randomly selected in the following experiments. For each experiment ≥ 3 independent biological replicates were used (i.e. cells derived from 3 or more different donor dogs).

Cell isolation and cell culture

Before excision, the eyes were examined using a handheld slit lamp (KOWA SL14, Kowa Company LTD, Naka-ku, Nagoya, Aichi, Japan) by a board-certified veterinary ophthalmologist (CK).

Within an average time of 8.28 ± 3.38 h after confirmed death the cornealscleral buttons were excised. Left and right eyes were placed in separate containers containing Eagle's Minimum Essential Medium (Sigma-Aldrich, Gillingham, Dorset, UK), 5% dextran (Sigma-Aldrich), 2% foetal bovine serum (Gibco, Life Technologies, Paisley, UK) and 1% Antibiotic-Antimycotic mix (Sigma-Aldrich) at room temperature for an average time of 13.5 ± 6.38 days (range: 6-21days) with a weekly change of the media.

The CSCs were isolated using a method similar to that described previously [12]. Briefly, with magnification of 5.5x surgical loupes (Keeler, Winsdor, UK), the superficial corneal limbal region was excised using a 300 μm set depth knife (BD, beaver visitec international, Bidford-Upon-Avon, Warwickshire, UK). The limbal anterior stroma including the epithelium was removed using corneal scissors and dissected into small fragments (3x3mm). The central cornea was trephined using a 7.5 mm corneal hand-held trephine (Altomed, Bolden, UK) and dissected into strips using a 300 μm set depth knife. The limbal and central tissue fragments of each donor were processed separately and digested in 50% Dulbecco's Modified Eagle's Medium (DMEM) high glucose (Gibco), 50% DMEM/F12 (Gibco), supplemented with 50 $\mu\text{g}/\text{mL}$ gentamicin (Gibco), 1% Penicillin-Streptomycin solution (Gibco), containing type L collagenase from *Clostridium histolyticum* (0.5 mg/mL ; Sigma-Aldrich) and incubated at 37°C, 5% CO_2 for 12-14 h. Selective trypsinization was used (TripLE express; Gibco) to separate the small oval shaped CSC from epithelial cells, keratocytes and melanocytes. CSCs were expanded to a maximum confluency of 60-70%. The medium was changed every 48-72 hours. CSC medium was composed of DMEM low glucose (Gibco) and MCDB-201 (Sigma-Aldrich) medium, 10 ng/mL epidermal growth

factor (EGF) (Sigma-Aldrich), 10 ng/mL platelet-derived growth factor (PDGF-BB; R&D Systems, Abingdon, Oxford, UK), Insulin-Transferrin-Selenium (Gibco), 0.1 mM ascorbic acid-2-phosphate (Sigma-Aldrich), 10^{-8} M dexamethasone (Sigma-Aldrich), 1% Penicillin-Streptomycin (Gibco), 50 ug/mL gentamicin (Gibco), 100 ng/mL cholera toxin (Sigma-Aldrich), supplemented with 2% fetal bovine serum (FBS) (Invitrogen, Thermo-Fisher Scientific, Paisley, UK) [15].

Population doubling time and population doublings

The mean population doubling time (PDT) was calculated from three biological independent limbal and central derived CSC lines (8 year old Springer Spaniel (No. 10), 12 year old Lurcher (No.11), 12 year old Golden Retriever (No. 12), Supplementary table 1). The doubling time and number of cell doublings was calculated at each passage until the stationary phase was reached (P1-P6). (Roth V. 2006 Doubling Time Computing, Available from: <http://www.doubling-time.com/compute.php>)

The population doubling of cells was calculated as: Number of Cell Doublings (NCD) = $\log_{10}(y/x)/\log_{10}2$, where “y” is the final density and ‘x’ is the initial seeding density of the cells [10].

The cell number of P0-P1 was not included as CSC derived from cultured limbal and central cells had epithelial cell contamination.

Keratocyte differentiation of CSCs

Limbal and central derived CSCs (passage 2-5) of a 12 year old Lurcher, (No.11), 12 year old Golden Retriever (No. 12), and a 2 year old Border Collie (13) (see Supplementary table 1) were cultured in keratocyte differentiation medium (KDM) consisting of advanced DMEM (Sigma-Aldrich), 10 ng/mL human basic fibroblast growth factor (bFGF) (Sigma-Aldrich), 0.1 mM L-ascorbic acid-2-phosphate (Sigma-Aldrich), 50 ug/mL gentamicin (Invitrogen), 1% Penicillin-Streptomycin (Gibco), 1% Gluta-MAX (Gibco). Medium was changed every 2-3 days. Cells of each donor and location (limbal/central) were cultured separately. A seeding density of 1×10^3 cells/cm² and one passage between 10-14 days was necessary to maintain stellate cell morphology, avoid cell confluency and cell sheet formation. A second culture experiment was conducted with the same media but lacking human bFGF (Sigma-Aldrich).

Cell culture of adipose-derived mesenchymal stem cells

Three lines of canine adipose-derived MSCs (adMSC) that had been derived previously were used as positive controls (11 year old Mix breed (No. 15) ,8 year old Irish setter (No. 16), 6 weeks old Dalmatian (No. 17) (see Supplementary table 1)) [22]. The cryopreserved MSCs were thawed into DMEM (Gibco) with 10% FBS (Gibco), 1% Penicillin-Streptomycin (Gibco) and 2 mM L-glutamine (Gibco). Media was replaced every 2-3 days. MSCs were used between passages 2-5.

Histology, Immunohistochemistry and Immunofluorescence staining

Three corneas from biological independent donors (1.2 year old (no.1), 1.3 year old (no.2) and 1.5 year old (No.3) Staffordshire bull terrier, see Supplementary table 1) were embedded in O.C.T. tissue compound (Tissue Tek®, VWR, Lutterworth, Leicestershire, UK). The tissue was separated in the dorsal, temporal, ventral and nasal regions, snap frozen in liquid nitrogen and cut in 7 µm thick frozen sections for routine automated Haematoxylin-Eosin and Periodic Acid Schiff (PAS) staining. Immunohistological investigations were performed on each of the four indicated regions.

The sections were fixed in 3% paraformaldehyde for 20 min., washed in PBS and permeabilized in 0.1% Triton-X100 (Sigma Aldrich) in PBS for 20min.

Limbal and central CSCs, their differentiated keratocyte-like cells (KDCs) from three different donors (12 year old Lurcher (No.11), 12 year old Golden retriever (No. 12), 2 year old Border collie (No. 13), see Supplementary table 1,) and adMSCs were plated onto Fibronectin (FNC coating mix, Athena Enzyme systems™, Baltimore, USA) coated permanox slides at a density of 4×10^4 cells/slide, cultured for a 2-3 days in CSC, MSC (at passage 2–5) or keratocyte differentiation media (KDM), fixed with 3% paraformaldehyde for 20 minutes. For sections and fixed cells prepared for identification of keratocyte markers, 0.1% Tween 20 (Sigma-Aldrich) in PBS was used for washing procedures. Cells/sections were blocked with 10% goat/donkey serum (Sigma-Aldrich) in PBS for 60 minutes at room temperature (RT). Details of primary and secondary antibodies are summarized in supplementary table 2. Briefly, the cells/sections were incubated with the primary antibody in 5% blocking serum (goat or donkey serum (both Sigma-Aldrich) in PBS

at 4°C overnight. Slides were washed in PBS and incubated with corresponding secondary antibody diluted in 5% blocking serum in PBS for 1 hour at RT and FITC-labelled phalloidin (1:1000 concentration; Sigma-Aldrich), which binds to the actin cytoskeleton, mounted in Vectashield with the nuclear stain DAPI (Vector laboratories Inc., Peterborough, UK) and evaluated with a confocal microscope (Zeiss LSM 700, Cambridge, UK). Rabbit and Mouse IgG isotype controls were performed.

Flow Cytometry

Flow cytometry was performed on three independent biological replicates of limbal CSCs (12 year old Lurcher (No.11), 12 year old Golden retriever (No. 12), 2 year old Border collie (No. 13) Supplementary table 1,). Cells were fixed in 3% paraformaldehyde (Sigma-Aldrich) for 20 minutes prior to washing, permeabilized in 0.1% Triton x-100 for 1 h (except for CD90) and blocked in 10% goat or donkey serum (Sigma-Aldrich) for 30 min. Cells (1×10^6) were incubated for 45 min at 4°C with primary antibody, rabbit or sheep IgG, followed by incubation with the appropriate FITC labeled secondary antibody for 45min 4°C. Details of all primary and secondary antibodies used for immunostaining are listed in supplementary table 2.

A FACS Calibur flow cytometer (BD Biosciences Immunocytometry Systems, Franklin Lakes, NJ) was used and the data were analyzed using Novoexpress[®] Software (ACEA Biosciences, San Diego, USA). Events were gated to exclude dead cells and cell debris by forward versus side scatter height (R1). R1 events were gated to remove doublets (R2) by forward scatter height versus forward scatter area. 2% of events in the R2 isotype control and everything to the right were included in a new gate (R3) by FITC height versus forward scatter height [23]. The overlaid events of each primary antibody gated within R3 were considered positive. The events were expressed as means of positive cells (%).

RNA extraction and Quantitative Reverse Transcriptase Polymerase Chain Reaction

Total RNA was extracted from corneal tissue, 1×10^6 limbal CSC (passage 4-5) and 1×10^6 of their KDC of three different donors (12 year old Lurcher (No.11), 12 year old Golden retriever (No. 12), 2 year old Border collie (No. 13), see Supplementary table 1,) using Tri- reagent (Sigma-Aldrich), purified using the RNeasy mini kit (Qiagen, Germantown, USA)

and treated with Ambion DNA-free (Life Technologies) to remove genomic DNA. cDNA was made from 1 µg of RNA using the sensiFAST cDNA synthesis kit (Bioline, London, UK). Aliquots of 2 µl cDNA were used in qPCR, which was carried out using SYBR Green containing supermix (Bioline) on the Bio-Rad C1000 Touch Thermal Cycler (Bio-Rad, Watford, UK). QPCR reactions were performed in duplicate. The cycle parameters were 95°C for 10 min, followed by 40 cycles of 95°C for 15 s, 60°C for 15 s and 72°C for 15 s. Finally, a melt curve was produced by taking readings every 1°C from 65°C to 95°C. The levels of canine 18S rRNA did not change between treatments (data not shown) and it was used to normalize gene expression using the $2^{-\Delta\Delta C_t}$ method [24].

Primers were designed from annotated canine exon sequence for the genes of interest using primer3 (<https://primer3.org/webinterface.html>) and mfold (<http://unafold.rna.albany.edu/?q=mfold>) software to obtain amplicons with a melting temperature (T_m) of 58°C – 62°C, devoid a secondary structure at T_m 60°C and with an amplicon size of 50-150 bp. Primers were produced by Sigma-Aldrich. Primer sequences can be found in the Supplementary table 3.

Assays for Adipogenesis, Osteogenesis and Chondrogenesis

Central (donor: 6 weeks old Dalmatian (No. 8), 8 weeks old Old english sheepdog (No. 9), 12 year old Golden Retriever (No. 12), 2 year old Border Collie (No. 13) and limbal (donor: 1 year old Staffordshire cross breed (No. 6), 8 week old Old english sheepdog (No. 9), 12 year old Lurcher (No. 11), 2 year old Border Collie (No. 13) derived CSC and adMSC from three different donors of passage 2-5 (see Supplementary table 1) were differentiated into adipocytes, chondrocytes and osteoblasts. The following modified protocols by Guest et al. 2008 were used [25]. For adipogenic differentiation CSC and adMSC were treated with antibiotic-free fat induction media (DMEM supplemented with 10% foetal calf serum, 15% rabbit serum (Invitrogen), 10 µg/ml insulin, 1 µM dexamethasone, 0.02 mM indomethacin, and 0.5 mM 3-isobutyl-1-methylxanthine (Sigma-Aldrich) for 72 hours and followed by antibiotic-free fat maintenance media (DMEM supplemented with 10% fetal calf serum and 10 µg/ml insulin) for 72 h for three alternating cycles. Oil red O staining for lipid droplets was then carried out.

For chondrogenic differentiation cells were treated with cartilage induction media (DMEM supplemented with 10% foetal calf serum, 2 mM L-glutamine, 100 U/ml penicillin, 100 µg/ml streptomycin, 1×10^{-7} M dexamethasone (Sigma) and 15 ng/ml TGF- β 1 (Peprotech, London, UK) for 21 days. Alcian blue staining (pH 1.0) was carried out overnight and short nuclei counterstain in 0.5% aqueous neutral red (30 sec) was performed. This was performed in 2D (biological triplicate) and 3D (biological singlicate) pellet form using a starting density of 1×10^6 cells. The pellet was embedded in Tissue Tek® O.C.T. compound and 10µm frozen sections stained accordingly.

For osteogenic differentiation cells were cultured for 21 days in osteogenic induction media (DMEM supplemented with 10% foetal calf serum, 2 mM L-glutamine, 100 U/ml penicillin, 100 µg/ml streptomycin, 10 mM β -glycerophosphate (Sigma), 10 nM dexamethasone and 0.1 mM ascorbic acid (Sigma) before staining with von Kossa (Abcam, Cambridge, UK), Alizarin red S (Sigma) and inorganic hydroxyapatite stain (OsteoImage™ Mineralization Assay, Lonza®, Walkersville, USA) according to the manufacturer's instructions. The human sarcoma osteogenic cell line (SAOS-2) served as positive control.

Western Blot analysis

Antibodies without canine specific references were tested for cross-reactivity and specificity to dog proteins using western blot. Details are in supplementary table 2.

Protein was extracted from whole cell extracts (WCEs) from adMSC (P4), CSC (P4) and corneal tissues using 500 µl WCE buffer (5 mM EDTA, 5 M NaCl, 0.5 M HEPES pH7.9, 100 mM PMSF), followed by three freeze and thaw cycles. Supernatants were collected by centrifugation at 4°C and stored at -20°C.

To test the keratocyte markers Lumican and Keratocan, a deglycosylation step was performed using a combination of endo- β Galactosidase (Sigma-Aldrich) (0.57 Units/mg protein for 4 h at 37°C) and Chondroitinase ABC (Sigma-Aldrich) (0.6 Units/mg protein) for 4 h at 37°C on 100 µg of corneal protein. 20 µg of denatured protein was run either on a 10% or 5% SDS-polyacrylamide gel and transferred to a PDVF membrane. Immunoreactivity was detected using the ECL plus detection system (Amersham,

Buckinghamshire, UK). Mouse anti- β actin antibody (Abcam) was used as a positive control.

PBMC media and isolation from lymph nodes

The rapid destruction of peripheral blood PBMCs through the use of commercial euthanasia agents prevented the isolation of PBMCs from the blood of the euthanized patients from the corneal donor study population.

Therefore, the popliteii lymph nodes of two donor dogs were harvested 2 hours after euthanasia and transported on ice in PBMC media as described by Dutton et al 2018 [26]. PBMC media was composed of RPMI 1630, 10% heat inactivated FBS, 1% Penicillin-Streptomycin (Gibco), 2 mM L-glutamine and 55 μ M 2- β mercaptoethanol (all Sigma-Aldrich).

Briefly, lymph nodes were excised, cut into small pieces and passed through a 70 μ m sterile cell strainer (Sigma-Aldrich) followed by several washes. The cell suspension was centrifuged at 300 G for 15 minutes and cells were frozen in liquid nitrogen a concentration of 4×10^6 /ml in 90% PBMC media and 10% DMSO. After thawing 77-95% of PBMCs were viable.

Canine PBMCs of two dogs were commercially purchased (3H Biomedical, Uppsala, Sweden).

PBMC co-cultures

CSCs were growth arrested with 15 μ g/ml (2 hour incubation) Mitomycin C (MMC) (Sigma-Aldrich). PBMC co-cultures were performed by incubating growth arrested, allogeneic CSC on a 96 well plate with effector PBMCs of two different donors in a ratio of 1:5 (CSC: PBMC). The experiment was performed on three biologically independent limbal CSCs from three different donors (donor: 1.3 year old Staffordshire bull terrier (No 2), 1.5 year old Staffordshire bull terrier (No. 3), 12 year old Golden retriever (No.12), see Supplementary table 1), (i.e. CSCs of three different donors were used with two different PBMC donors)). For the negative controls, PBMCs were MMC treated for 30 minutes at a

concentration of 50 µg/ml before being washed and cultured with autologous effector PBMCs.

For positive controls, growth arrested PBMCs were cultured with allogeneic effector PBMCs. Additionally, PBMCs were activated with 10 µg/ml Phytohemagglutinin (PHA, Sigma-Aldrich).

After 4 days the PBMCs were incubated with radioactive thymidine ($[^3\text{H}]$ thymidine) (GE Healthcare Bio-sciences) at a final concentration of 0.5 µCi per well, at 37°C, 5% CO₂ for 16-18 hours before being frozen at -20°C. Following thawing, cells were harvested using a Filtermate and counted using Topcount NXT equipment.

Statistical Analysis

Statistical analyses of the cell culture kinetics and gene expression data followed a normal distribution calculated by Shapiro-Wilk normality test (W) and p values >0.05 (XLSTAT-base, Wittenhausen, Germany). Group differences were calculated using an unpaired Student's t -test and $p < 0.05$ was considered to be statistically significant.

Results

The canine limbus has epithelial invagination and an undulating basement membrane. A distinct population of corneal stromal cells in the limbus and central stroma express the mesenchymal stem cell marker CD90.

By histology, limbal crypts and palisades of Vogt (as in humans) were absent in canines (Fig.1B), however a slight invagination of the epithelium in the stroma was noted. In the canine corneal limbus, the basement membrane was undulated and irregularly formed. There was no evidence of regional differences (dorsal, ventral, nasal, temporal). In the limbus, the basal cell layer of the epithelium was cell rich with more elongated basal cell nuclei similar to limbal epithelial stem cells (LESC). The corneal stromal cells were in direct contact or in close proximity to the irregular formed basement membrane (Fig. 1B). A distinct, small population of these stromal cells expressed CD90 and extended into the mid-stroma of the limbal region in all four quadrants (Fig. 1B).

In the central cornea, the basal cells of the epithelium were cuboidal in shape. The fine basement membrane was regularly formed and the stromal cells were separated from the basement membrane by a layer of corneal stroma (Fig.1C). A distinct population of stromal cells expressing CD90 extended into the mid-stroma (Fig. 1C). Pax6 expressing stromal cells were not evident in the limbal or the central cornea.

CSCs can be cultured in vitro from both the limbal and central cornea but have a limited self-renewal

Adherent cells were visualised approximately six hours post seeding. The cells adopted an ovoid morphology after 24 h but after the first passage, they showed a more spindle cell morphology and formed a syncytium of spindle cells with increasing confluency (Fig.2 Ai-iii).

The average maximum passage was 9 (± 2.94) and 8 (± 1.64) ($P = 0.55$) passages over a culture time of 23.5 (± 3.31) and 19.6 (± 4.33) days ($P = 0.18$) in limbal and central derived CSCs respectively (Fig. 2B). There were no statistically significant differences in cell numbers of the limbal and central CSCs over 6 passages ($P = 0.54$ (P1), $P = 0.67$ (P2), $P = 0.83$ (P3), $P = 0.12$ (P4), $P = 0.49$ (P5), $P = 0.44$ (P6)) (Fig. 2C). The mean population doubling times between limbal and central derived CSC showed a trend that central CSC reached the stationary phase at an earlier passage (P3-4) than the limbal CSC, but the difference did not reach statistical significance ($P = 0.068$) (Fig. 2D). In the early log-phase, between P1-2, a PDT of 25.02h and 21.67h of limbal and central derived CSCs respectively were noted, which increased exponentially and reached the stationary phase after five passages for both central and limbal CSCs (Fig. 2D). The accumulative number of cell doublings between P1-P5 was 12.84 and 11.15 in limbal and central CSCs respectively (Fig. 2E).

Canine CSCs have mesenchymal stromal cell characteristics

Cultured limbal and central derived CSCs both expressed MSC markers. CSC showed strong expression of CD90 and CD73, whereas CD105 was less intensely expressed (Fig. 3). The nuclear paired box protein Pax6 (oculorhombin) and the intercellular membrane marker N-cadherin were expressed (Fig. 3). CD34, a haematopoietic stem cell marker and alpha smooth muscle actin (α -SMA), a myofibroblast marker were absent (Fig.3).

Canine adMSCs were used as a positive control and showed a similar marker expression to CSCs but lacked expression of Pax6 and CD34 and had strong expression of α -SMA (Fig. 3).

Flow cytometry revealed that 83% of CSCs expressed Pax6, 96% expressed CD90 and CD73 whereas 1% expressed CD34 (Fig. 4).

Western blot analysis confirmed the specificity and cross reactivity of the antibodies to the dog proteins for Pax6, N-cadherin, CD90, CD73 (supplementary figure 1).

Furthermore, CSCs could differentiate into bone, fat and cartilage producing cells demonstrating their multipotency (Fig 5). Whilst there were no apparent differences in the high efficiency of CSC and MSC differentiation into adipocytes (Fig. 5 A vii,viii), the bone differentiation showed a moderate osteogenic response in both, CSCs and adMSCs (Fig. 5 A i-vi) (compare to Supplementary figure 2). CSC differentiation into cartilage 3D (Fig. 5 B i-iv) and 2D (Fig. 5 B v,vi) required a higher concentration of TGF β 1 than that used for MSC differentiation (15 ng/ml versus 10 ng/ml).

CSCs are immune privileged in vitro

Allogeneic limbal CSC co-cultured with effector PBMCs did not modify the baseline level PBMC proliferation. In comparison co-cultures of effector PBMCs with allogeneic PBMCs showed a significant ($P < 0.001$) increase in proliferation compared to non-activated PBMC (Fig. 6).

CSC differentiate into keratocyte-like cells and bFGF plays an essential role in the down regulation of α -SMA

Limbal and central derived CSCs were cultured under low glucose, serum-free conditions with substituted ascorbic acid to induce their differentiation into keratocytes (KDM). The small, polygonal morphology characteristic of CSCs changed to a stellate morphology typical of keratocytes within 7-10 days (Fig. 7 A). A seeding number of 1×10^3 cells/cm² differentiated in KDM containing human bFGF with an additional passage step maintained keratocyte marker expression without the expression of α -SMA over 21 days. Keratocyte-like cells showed increased protein expression of Lumican, Keratocan and ALDH1A3, whereas Pax6 expression decreased and N-cadherin expression became undetectable following differentiation (Fig. 7 B). This was reflected in the fold change in gene expression

of KDCs to undifferentiated CSCs where *Keratocan* was significantly upregulated ($P < 0.05$). *Lumican* ($P=0.27$) and *ALDH1A3* ($P=0.21$) were also upregulated following differentiation but did not reach significance. In contrast the stem cell associated genes, *Pax6* ($P=0.077$) was downregulated and *N-cadherin* ($P < 0.0001$) was significantly downregulated (Fig. 8 A).

A-SMA is a myofibroblastic marker, which is minimally expressed at the gene level and not detected at the protein level in undifferentiated CSCs (Fig. Fig. 8 B i, C) or following keratocyte differentiation in the presence of bFGF (Fig. 8 Bii, C). However, in the absence of bFGF, α -SMA gene is significantly upregulated ($P < 0.001$) and protein expression are detected in the differentiated cells (Fig. 8 B iii, C).

Western blot analysis confirmed the specificity and cross reactivity of the antibodies to the dog proteins for Lumican, Keratocan and ALDH1A3 (Supplementary Fig.1).

Discussion

The corneal limbus in humans is located in the junction between the cornea and the sclera. In humans, the limbus is composed of limbal crypts and Palisades of Vogt which serves as a stem cell niche, for limbal epithelial stem cells (LESCs), which are responsible for self-renewing and repair of damaged corneal epithelium [27]. The loss of LESCs results in Limbal Stem Cell Deficiency (LSCD), and leads to inflammation, scarring, neovascularisation and possible blindness [28]. The fate of LESCs within their niche is influenced by the stromal microenvironment. In humans, limbal stromal cells have MSC characteristics and are described as corneal stromal stem cells (CSSC) [29,30] or limbal MSCs (L-MS) [9,10]. In humans, these stromal cells are hypothesized to assist in the maintenance of the LESC niche [31].

This is the first description of limbal and central derived corneal stromal cells with multipotent MSC characteristics in dogs, similar to those described in humans [7,8,12,20,32]. We also provide essential baseline data of the limbal anatomy in dogs.

A major anatomical difference to humans was the absence of limbal crypts and palisades of Vogt [33]. We can also confirm a slight invagination of the epithelium in the stroma as described by Patrino et al 2017 [33]. Well-defined palisades of Vogt are present in the pig eye but reportedly absent in rabbits and rodents [34,35].

Immunohistologically, a small population of CD90 expressing stromal cells in the limbal and central anterior corneal stroma was present. CD90 is a well-accepted MSC marker, however, it can also be expressed by fibroblasts [11]. To characterise the CD90+ cell population in more detail, double or even triple IHC using CD90, α -SMA and Vimentin should be included in future studies. Canine MSCs are characterized in the veterinary field, including adipose derived, bone marrow derived MSC's and other tissue sources as amniotic-derived, synovial –derived, periosteum [36-42]. The international society for cellular therapy (ISCT) has defined a set of criteria that must be established to be characterized as a multipotent mesenchymal stromal cell [11]. Canine MSCs studies fulfilled these criteria, however positive and negative MSC marker profiles differ in various studies, some studies also demonstrated cells were positive for the pluripotency- associated genes NANOG, OCT4, and SOX2 [41,43]. Canine MSCs are not a homogenous cell population. Hence, proliferation capacity has been reported to be lower in bone marrow (BM)-MSCs in contrast to adMSCs and synovial MSCs [37,41]. Proliferation is also lower in MSCs isolated from older donors, “stemness” can decrease with passage frequency and the harvest site can have significant impact [43,44]. Breed related differences have also been described. For example BM-MSCs of Howavart's had significantly less colony forming units (CFU) than German Shepherd, Flat coated Retriever or Golden Retriever [45]. Therefore had human MSCs culture protocols adjusted to canine MSCs [42,46,47].

This is the first report of canine MS-like cells of corneal origin and therefore the results are primarily compared to human corneal stromal MSC studies. The CSCs are isolated and cultured using different culture conditions to MSCs and therefore more detailed comparisons to canine MSCs in terms of culture conditions, cell proliferation, marker expression and differentiation potential may be beneficial in future work.

Funderburgh et al 2005 described a small population of limbal stromal cells expressing the transcription factor Pax6 (oculorhombin) in bovine corneas [7]. This could not be confirmed histologically in canine corneas [8].

Stromal cells from the canine limbal and central cornea were successfully isolated and cultured. Differential trypsinisation of small polygonal cells, which reached a maximal

confluency of 60-70%, allowed the selective culture of CSC. A stem cell like appearance could largely be maintained throughout several passages [15]. CFU-f assay of limbal and central CSCs as shown human limbal CSSC was not performed but should be included in future studies [9,10,48]. In contrast to Du et al 2005, selective cell sorting to expand a CSSC “side population” was not performed [12]. This approach in human cells, which used the same low serum CSSC culture media than in the present study, resulted in a population with a replicative lifespan typical of stem cells (18 passages and a cumulative population doubling of 80 until senescence was reached) [12]. Human CSC populations cultured in 10% containing FBS without growth factor (EGF, PDGF), isolated without cell sorting produced more limited replication with 22.9 cell doublings between passages 2-6 (higher than in dogs). However, a PDT of 29.1h and 34.1h similar to human MSC was observed only at early passages, similar to the present study [10].

Canine CSC underwent 12 and 11 population doublings for the limbal and central derived CSC respectively over 5 passages until senescence was reached. A population doubling time of approximately 24-30h as described in canine MSCs was only reached in the early log-phase (P1-P2) [36]. Guercio et al 2013 also reports a limited life-span and senescence after passage 6 in canine adMSC (cultured in DMEM low glucose, 20% FBS) and revealed similar accumulated PD (11-12) in a similar time (27-28 d) to the present study of CSC. Bearden and colleagues 2017 showed that adipose and synovium canine MSCs proliferated first more rapidly with a rapid decline after passage 3, than marrow cMSCs, which we could very similar observed in CSC. However, we hypothesis that the limited self-renewal of CSC population in dogs may suggest they are proliferating progenitor cells rather than stem cells or might resemble a mixed population of cells [49]. Hence, the term canine CSC was used instead of CSSC as in humans. The corneal stem cell media could also influence the degree of self renewal and might require optimization to the canine species in future studies. CSSC media contains only low serum levels of 2% FBS and not 10% or higher as in most canine MSC culture conditions . This was performed as higher serum concentrations have been shown to induce a myofibroblastic cell fate in rabbit keratocytes [50]. Serum supplementation (10% v/v) led to human keratocyte differentiation into fibroblasts with loss of keratocan expression in human CSSC [12-14]. Whether this holds true for canine keratocytes and canine CSC is unknown. The CSSC media also contains the growth factors

EGF and platelet derived growth factor (PDGF) It is described that factors as FGF, TGF- β , PDGF, insulin-like growth factor 1 (IGF-1) and EGF regulate keratocyte differentiation, migration and expression and are known to be essential growth factors in corneal *in vitro* studies [51,52]. A canine study of BM-MSCs reported that cells expanded best in a-MEM supplemented with bFGF [45] and future studies to optimise canine CSC media to maximise self-renewal and differentiation potential are required.

No significant differences in culture kinetics were observed between limbal and central derived CSCs, although the central CSC showed a trend towards lower frequency of passage, lower cell numbers and earlier senescence. There was a high degree of heterogeneity in cell expansion which might be explained by the wide age range of donor tissue (0.2-12 years) that was used in this study, Comparative studies of the influence of age on human CSCs which are isolated and cultured similar to canine CSC in the present study are lacking. However, donor age can negatively impact human and canine MSC cell expansion and differentiation [44,53].

Effects of age in skeletally immature (mean age: 4.9 ± 1.9 months) and mature (mean age: 89.5 ± 20.9 months) dogs on canine BM-MSCs were studied by Volk and colleagues 2012. BM cells were isolated from long bones (humeri, femurs, and tibias) and cultured in high glucose DMEM substituted with 10% FBS, showed a significant negative effect of age on both MSC frequency and the ability to differentiate along the osteogenic lineage [44]. Guerico et al (2013) compared the age (young dogs: 1–4 years; adult dogs: 8–14 years) and the harvest site (subcutaneous versus visceral) of adMSCs cultured in low glucose DMEM and 20% FBS. Population doubling values at passages >2 were significantly higher for MSCs derived from subcutaneous fat and in younger dogs. CFU-f assay in low glucose DMEM and 5% FBS did not differ according to age and harvest location site, but declined after passage > 2.

The influence of donor age on cell expansion and differentiation of canine CSCs warrants further investigation in future studies.

We were able to differentiate both limbal, central derived CSC and adMSC into chondrogenic, adipogenic and osteogenic cells *in vitro*. However, It should be noted that canine chondrogenesis in MSC has not been robustly demonstrated in the literature and

difficulties in establishing a protocol are described [37,42]. In order to successfully drive chondrogenic differentiation of the CSCs, we had to use an increased concentration of TGF- β 1 compared to the MSCs. However, further optimization of the differentiation protocol could be performed [41] or a standardized commercial available differentiation media could be tested in future studies [43]. The induction of the osteoblastic lineage was demonstrated using a combination of van Kossa (mineralization –phosphate) and Alizarin S red (calcium) and hydroxyapatite staining but differentiation was not as robust when compared to SAOS-2 cells (see Supplementary figure 2). Passage number, pluripotency gene expression [43] and donor age have all been shown to affect the differentiation capacity of canine MSCs and were not tightly controlled in the present study (cells were at passage 2-5 and from donors aged 0.2-12 years). Future work could also optimise the osteogenic differentiation protocol, for example thorough the addition of BMP-2 or IGF-1 [41,47,54].

The immunophenotyping of limbal and central derived CSC showed remarkable similarity with the surface antigen profile of adMSC for CD90, CD73, CD105, N-cadherin and CD34. In contrast to most human studies characterizing limbal CSCs, the present study used a limited number of protein markers; however, this reflects the nature of establishing protocols for the use of markers on canine tissue and cells. Most of the markers are not established in this species and therefore, western blot analysis had to confirm the specific binding.

The expression of CD34 in human CSSCs and keratocytes is controversial in human corneal research. CD34 is a hematopoietic stem cell surface marker, which is defined to be absent (<2%) in MSCs [11]. This was also confirmed for human limbal and central CSSCs [8,10].

CD34 has been described as a characteristic marker of quiescent keratocytes in the human cornea [56]. Another study characterizing limbal MSCs showed a drop of CD34 marker expression with increasing cell proliferation and a shift to more progenitor cell type. This seems to be influenced significantly by the composition of culture media [9,57,58]. In our study we found CD34 protein expression in less than 2% of canine CSCs. Canine adMSC in the present study also did not express CD34, which is similar to other reports for canine MSCs [36-38].

In contrast to CSCs, adMSC did not express Pax6, which was not expected given their origin. However, adMSC did express α -SMA which was not detected at the protein level in undifferentiated CSCs. α -SMA expression has been reported in human, rat and murine MSCs previously [59-61].

Alpha-SMA, the earliest known protein expressed in differentiation of the smooth muscle cells during development and is also transiently expressed by a variety of mesodermal cells during development, tissue repair, and neoplastic growth [61]. Tissue repair and tumor microenvironment can convert MSCs into contractile myofibroblasts (MF) that form α -SMA-containing stress fibers [62,63]. MF activation is part of the wound healing response, but persistent MFs contribute to fibrosis by excessively producing and contracting collagenous extracellular matrix (ECM) into stiff scar tissue [63].

Human CSCs have been shown to not only fail to induce the proliferation of allogeneic PBMCs but actually suppress the proliferation of activated PBMCs *in vitro* [8]. We have demonstrated that canine CSCs also appear to be immune privileged *in vitro* as they fail to induce the proliferation of PBMCs isolated from different donors. We carried out these assays on three different lines of CSCs each using PBMCs from two different donors (with PBMCs isolated from both lymph nodes and commercial suppliers) and all replicates produced very consistent results. However, the cells were not typed for dog leukocyte antigens (DLA) and therefore we cannot rule out the possibility that the cells were not true-mismatches. Further work is also required to determine if the CSCs are immune suppressive.

Canine CSCs (limbal and central) were successfully differentiated into cells with stellate keratocyte typical morphology that expressed keratocyte markers Keratocan, Lumican and ALDH1A3 [15,64,65]. ALDH1A3 is expressed in the murine cornea and is also required for corneal maintenance [66,67]. Similar to human studies, we could demonstrate that the gene expression levels of stem cell markers were downregulated and keratocyte markers were upregulated after 21 days of differentiation [12,68].

Canine CSCs continued to proliferate during the keratocyte differentiation process which might be driven by bFGF [69]. Therefore, KDM without bFGF was tested which led to stable cell numbers during differentiation. Although the absence of bFGF during the

differentiation had no influence on keratocyte marker expression, it did lead to a significant increase in α -SMA gene expression and the induction of detectable levels of protein. BFGF has been shown to downregulate α -SMA expression in adMSCs previously [70]. In the injured cornea, keratocytes differentiate into myofibroblasts in response to TGF β 1 [71]. To date, the reverse process turning myofibroblasts into keratocytes has not been described [72]. From a translational medicine perspective, using α -SMA expressing cells *in vivo* should be further investigated carefully.

In conclusion, the limbus of dogs lacks limbal crypts as in humans but has an undulating basement membrane with CD90+ stromal cells in close proximity to the limbal epithelium. For the first time we characterize a cell population in the canine corneal stroma (limbal and central) that contains MSC-like cells similar to CSSCs in humans with keratocyte differentiation potential and possible immune privilege properties. This novel finding of corneal stromal cells with multipotent mesenchymal stromal cell properties will provide a baseline for researchers working with canine corneal disease models and for cell-based therapy in veterinary ophthalmology.

Acknowledgments

The authors would like to thank Dr Jan van Dijk for support with the statistical analysis and the Petplan Charitable Trust (S16-204-397), Bertie's Mission and the European College of Veterinary Surgeons for funding the work.

Author Disclosure Statement

No competing financial interests exist.

References

1. Murphy CJ, K Zadnik and MJ Mannis. (1992). Myopia and refractive error in dogs. *Invest Ophthalmol Vis Sci* 33:2459-63.
2. Shively JN and GP Epling. (1970). Fine structure of the canine eye: cornea. *Am J Vet Res* 31:713-22.
3. Morrin LA, GO Waring, 3rd and W Spangler. (1982). Oval lipid corneal opacities in beagles: ultrastructure of normal beagle cornea. *Am J Vet Res* 43:443-53.
4. Pascolini D and SP Mariotti. (2012). Global estimates of visual impairment: 2010. *Br J Ophthalmol* 96:614-8.
5. Robaei D and S Watson. (2014). Corneal blindness: a global problem. *Clin Exp Ophthalmol* 42:213-4.
6. Gelatt K, Brooks, DE (2011). Penetrating corneal grafts. Chapter 8: Surgery of the cornea and sclera. In: *Veterinary Ophthalmic Surgery*. Gelatt K, Gelatt JP ed. Saunders Elsevier, Philadelphia, USA. pp 223.
7. Funderburgh ML, Y Du, MM Mann, N SundarRaj and JL Funderburgh. (2005). PAX6 expression identifies progenitor cells for corneal keratocytes. *FASEB J* 19:1371-3.
8. Vereb Z, S Poliska, R Albert, OK Olstad, A Boratko, C Csontos, MC Moe, A Facsko and G Petrovski. (2016). Role of Human Corneal Stroma-Derived Mesenchymal-Like Stem Cells in Corneal Immunity and Wound Healing. *Sci Rep* 6:26227.
9. Branch MJ, K Hashmani, P Dhillon, DR Jones, HS Dua and A Hopkinson. (2012). Mesenchymal stem cells in the human corneal limbal stroma. *Invest Ophthalmol Vis Sci* 53:5109-16.
10. Polisetty N, A Fatima, SL Madhira, VS Sangwan and GK Vemuganti. (2008). Mesenchymal cells from limbal stroma of human eye. *Mol Vis* 14:431-42.

11. Dominici M, K Le Blanc, I Mueller, I Slaper-Cortenbach, F Marini, D Krause, R Deans, A Keating, D Prockop and E Horwitz. (2006). Minimal criteria for defining multipotent mesenchymal stromal cells. The International Society for Cellular Therapy position statement. *Cytotherapy* 8:315-7.
12. Du Y, ML Funderburgh, MM Mann, N SundarRaj and JL Funderburgh. (2005). Multipotent stem cells in human corneal stroma. *Stem Cells* 23:1266-75.
13. Foster JW, RM Gouveia and CJ Connon. (2015). Low-glucose enhances keratocyte-characteristic phenotype from corneal stromal cells in serum-free conditions. *Sci Rep* 5:10839.
14. Kureshi AK, M Dziasko, JL Funderburgh and JT Daniels. (2015). Human corneal stromal stem cells support limbal epithelial cells cultured on RAFT tissue equivalents. *Sci Rep* 5:16186.
15. Kureshi AK, JL Funderburgh and JT Daniels. (2014). Human corneal stromal stem cells exhibit survival capacity following isolation from stored organ-culture corneas. *Invest Ophthalmol Vis Sci* 55:7583-8.
16. Basu S, AJ Hertszenberg, ML Funderburgh, MK Burrow, MM Mann, Y Du, KL Lathrop, FN Syed-Picard, SM Adams, DE Birk and JL Funderburgh. (2014). Human limbal biopsy-derived stromal stem cells prevent corneal scarring. *Sci Transl Med* 6:266ra172. DOI: 10.1126/scitranslmed.3009644
17. Higa K, N Kato, S Yoshida, Y Ogawa, J Shimazaki, K Tsubota and S Shimmura. (2013). Aquaporin 1-positive stromal niche-like cells directly interact with N-cadherin-positive clusters in the basal limbal epithelium. *Stem Cell Res* 10:147-55.
18. Dziasko MA, HE Armer, HJ Levis, AJ Shortt, S Tuft and JT Daniels. (2014). Localisation of epithelial cells capable of holoclone formation in vitro and direct interaction with stromal cells in the native human limbal crypt. *PLoS One* 9:e94283.

19. Morgan SR, EP Dooley, C Kamma-Lorger, JL Funderburgh, ML Funderburgh and KM Meek. (2016). Early wound healing of laser in situ keratomileusis-like flaps after treatment with human corneal stromal stem cells. *J Cataract Refract Surg* 42:302-9.
20. Li H, Y Dai, J Shu, R Yu, Y Guo and J Chen. (2015). Spheroid cultures promote the stemness of corneal stromal cells. *Tissue Cell* 47:39-48.
21. Fernandez-Perez J, M Binner, C Werner and LJ Bray. (2017). Limbal stromal cells derived from porcine tissue demonstrate mesenchymal characteristics in vitro. *Sci Rep* 7:6377.
22. Baird A, T Barsby and DJ Guest. (2015). Derivation of Canine Induced Pluripotent Stem Cells. *Reprod Domest Anim* 50:669-76.
23. Overton WR. (1988). Modified Histogram Subtraction Technique for Analysis of Flow Cytometry Data. *Cytometry* 619-626.
24. Livak KJ, T.D. (2001). Analysis of Relative Gene Expression Data Using Real-Time Quantitative PCR and the $2^{-\Delta\Delta CT}$ Method. *Methods* 25:402-408.
25. Guest DJ, JC Ousey and MR Smith. (2008). Defining the expression of marker genes in equine mesenchymal stromal cells. *Stem Cells Cloning* 1:1-9.
26. Dutton LC, J Dudhia, B Catchpole, H Hodgkiss-Geere and D Werling. (2018). Cardiosphere-derived cells suppress allogeneic lymphocytes by production of PGE2 acting via the EP4 receptor. *8: 1335*. DOI:10.1038/s41598-018-31569-1
27. Secker GA and JT Daniels. (2008). Limbal epithelial stem cells of the cornea. In: *StemBook*. Cambridge (MA). pp DOI 10.3824/stembook.1.48.1.
28. Dua HS, JS Saini, A Azuara-Blanco and P Gupta. (2000). Limbal stem cell deficiency: concept, aetiology, clinical presentation, diagnosis and management. *Indian J Ophthalmol* 48:83-92.
29. Dziasko MA and JT Daniels. (2016). Anatomical features and cell-cell interactions in the human limbal epithelial stem cell niche. *Ocul Surf* 14: 322-330.

30. Hertszenberg AJ and JL Funderburgh. (2015). Stem Cells in the Cornea. *Prog Mol Biol Transl Sci* 134:25-41.
31. Poliseti N, P Agarwal, I Khan, P Kondaiah, VS Sangwan and GK Vemuganti. (2010). Gene expression profile of epithelial cells and mesenchymal cells derived from limbal explant culture. *Mol Vis* 16:1227-40.
32. Tomasello L, R Musso, G Cillino, M Pitrone, G Pizzolanti, A Coppola, W Arancio, G Di Cara, I Pucci-Minafra, S Cillino and C Giordano. (2016). Donor age and long-term culture do not negatively influence the stem potential of limbal fibroblast-like stem cells. *Stem Cell Res Ther* 7:83.
33. Patruno M, A Perazzi, T Martinello, A Blaseotto, E Di Iorio and I Iacopetti. (2017). Morphological description of limbal epithelium: searching for stem cells crypts in the dog, cat, pig, cow, sheep and horse. *Vet Res Commun* 41:169-173.
34. Notara M, S Schrader and JT Daniels. (2011). The porcine limbal epithelial stem cell niche as a new model for the study of transplanted tissue-engineered human limbal epithelial cells. *Tissue Eng Part A* 17:741-50.
35. Gipson IK. (1989). The epithelial basement membrane zone of the limbus. *Eye (Lond)* 3 (Pt 2):132-40.
36. Takemitsu H, D Zhao, I Yamamoto, Y Harada, M Michishita and T Arai. (2012). Comparison of bone marrow and adipose tissue-derived canine mesenchymal stem cells. *BMC Vet Res* 8:150.
37. Russell KA, NH Chow, D Dukoff, TW Gibson, J LaMarre, DH Betts and TG Koch. (2016). Characterization and Immunomodulatory Effects of Canine Adipose Tissue- and Bone Marrow-Derived Mesenchymal Stromal Cells. *PLoS One* 11:e0167442.
38. Kriston-Pal E, A Czibula, Z Gyuris, G Balka, A Seregi, F Sukosd, M Suth, E Kiss-Toth, L Haracska, F Uher and E Monostori. (2017). Characterization and therapeutic application of canine adipose mesenchymal stem cells to treat elbow osteoarthritis. *Can J Vet Res* 81:73-78.

39. Uder C, S Bruckner, S Winkler, HM Tautenhahn and B Christ. (2018). Mammalian MSC from selected species: Features and applications. *Cytometry A* 93:32-49.
40. Park SB, MS Seo, HS Kim and KS Kang. (2012). Isolation and characterization of canine amniotic membrane-derived multipotent stem cells. *PLoS One* 7:e44693. doi:10.1371/journal.pone.0044693
41. Bearden RN, SS Huggins, KJ Cummings, R Smith, CA Gregory and WB Saunders. (2017). In-vitro characterization of canine multipotent stromal cells isolated from synovium, bone marrow, and adipose tissue: a donor-matched comparative study. *Stem Cell Res Ther* 8:218.
42. Kisiel AH, LA McDuffee, E Masaoud, TR Bailey, BP Esparza Gonzalez and R Nino-Fong. (2012). Isolation, characterization, and in vitro proliferation of canine mesenchymal stem cells derived from bone marrow, adipose tissue, muscle, and periosteum. *Am J Vet Res* 73:1305-17.
43. Guercio A, S Di Bella, S Casella, P Di Marco, C Russo and G Piccione. (2013). Canine mesenchymal stem cells (MSCs): characterization in relation to donor age and adipose tissue-harvesting site. *Cell Biol Int* 37:789-98.
44. Volk SW, Y Wang and KD Hankenson. (2012). Effects of donor characteristics and ex vivo expansion on canine mesenchymal stem cell properties: implications for MSC-based therapies. *Cell Transplant* 21:2189-200.
45. Bertolo A, F Steffen, C Malonzo-Marty and J Stoyanov. (2015). Canine Mesenchymal Stem Cell Potential and the Importance of Dog Breed: Implication for Cell-Based Therapies. *Cell Transplant* 24:1969-80.
46. Schwarz C, U Leicht, C Rothe, I Drosse, V Luibl, M Rocken and M Schieker. (2012). Effects of different media on proliferation and differentiation capacity of canine, equine and porcine adipose derived stem cells. *Res Vet Sci* 93:457-62.

47. Volk SW, DL Diefenderfer, SA Christopher, ME Haskins and PS Leboy. (2005). Effects of osteogenic inducers on cultures of canine mesenchymal stem cells. *Am J Vet Res* 66:1729-37.
48. Li GG, YT Zhu, HT Xie, SY Chen and SC Tseng. (2012). Mesenchymal stem cells derived from human limbal niche cells. *Invest Ophthalmol Vis Sci* 53:5686-97.
49. Seaberg RM and D van der Kooy. (2003). Stem and progenitor cells: the premature desertion of rigorous definitions. *Trends Neurosci* 26:125-31.
50. Jester JV, PA Barry-Lane, HD Cavanagh and WM Petroll. (1996). Induction of alpha-smooth muscle actin expression and myofibroblast transformation in cultured corneal keratocytes. *Cornea* 15:505-16.
51. Kim A, N Lakshman, D Karamichos and WM Petroll. (2010). Growth factor regulation of corneal keratocyte differentiation and migration in compressed collagen matrices. *Invest Ophthalmol Vis Sci* 51:864-75.
52. Lakshman N and WM Petroll. (2012). Growth factor regulation of corneal keratocyte mechanical phenotypes in 3-D collagen matrices. *Invest Ophthalmol Vis Sci* 53:1077-86.
53. Choudhery MS, M Badowski, A Muise, J Pierce and DT Harris. (2014). Donor age negatively impacts adipose tissue-derived mesenchymal stem cell expansion and differentiation. *J Transl Med* 12:8. <https://doi.org/10.1186/1479-5876-12-8>
54. Levi B, ER Nelson, K Brown, AW James, D Xu, R Dunlevie, JC Wu, M Lee, B Wu, GW Commons, D Vistnes and MT Longaker. (2011). Differences in osteogenic differentiation of adipose-derived stromal cells from murine, canine, and human sources in vitro and in vivo. *Plast Reconstr Surg* 128:373-86.
55. Yamamoto M, HK Nakata, S.Hao, J., J Chou and S Kuroda. (2014). Osteogenic Potential of Mouse Adipose-Derived Stem Cells Sorted for CD90 and CD105 In Vitro. *Stem Cells Int* 2014:Article ID 576358. <https://doi.org/10.1155/2014/576358>

56. Joseph A, P Hossain, S Jham, RE Jones, P Tighe, RS McIntosh and HS Dua. (2003). Expression of CD34 and L-selectin on human corneal keratocytes. *Invest Ophthalmol Vis Sci* 44:4689-92.
57. Hashmani K, MJ Branch, LE Sidney, PS Dhillon, M Verma, OD McIntosh, A Hopkinson and HS Dua. (2013). Characterization of corneal stromal stem cells with the potential for epithelial transdifferentiation. *Stem Cell Res Ther* 4:75.
58. Sidney LE, MJ Branch, HS Dua and A Hopkinson. (2015). Effect of culture medium on propagation and phenotype of corneal stroma-derived stem cells. *Cytherapy* 17:1706-22.
59. Talele NP, J Fradette, JE Davies, A Kapus and B Hinz. (2015). Expression of alpha-Smooth Muscle Actin Determines the Fate of Mesenchymal Stromal Cells. *Stem Cell Reports* 4:1016-30.
60. Peled A, D Zipori, O Abramsky, H Ovadia and E Shezen. (1991). Expression of alpha-smooth muscle actin in murine bone marrow stromal cells. *Blood* 78:304-9.
61. Liu Y, B Deng, Y Zhao, S Xie and R Nie. (2013). Differentiated markers in undifferentiated cells: expression of smooth muscle contractile proteins in multipotent bone marrow mesenchymal stem cells. *Dev Growth Differ* 55:591-605.
62. Hinz B, G Celetta, JJ Tomasek, G Gabbiani and C Chaponnier. (2001). Alpha-smooth muscle actin expression upregulates fibroblast contractile activity. *Mol Biol Cell* 12:2730-41.
63. Hinz B, SH Phan, VJ Thannickal, M Prunotto, A Desmouliere, J Varga, O De Wever, M Mareel and G Gabbiani. (2012). Recent developments in myofibroblast biology: paradigms for connective tissue remodeling. *Am J Pathol* 180:1340-55.
64. Lakshman N, A Kim and WM Petroll. (2010). Characterization of corneal keratocyte morphology and mechanical activity within 3-D collagen matrices. *Exp Eye Res* 90:350-9.

65. Carlson EC, CY Liu, T Chikama, Y Hayashi, CW Kao, DE Birk, JL Funderburgh, JV Jester and WW Kao. (2005). Keratocan, a cornea-specific keratan sulfate proteoglycan, is regulated by lumican. *J Biol Chem* 280:25541-7.
66. Stagos D, Y Chen, M Cantore, JV Jester and V Vasiliou. (2010). Corneal aldehyde dehydrogenases: multiple functions and novel nuclear localization. *Brain Res Bull* 81:211-8.
67. Kumar S, P Dolle, NB Ghyselinck and G Duester. (2017). Endogenous retinoic acid signaling is required for maintenance and regeneration of cornea. *Exp Eye Res* 154:190-195.
68. Park SH, KW Kim, YS Chun and JC Kim. (2012). Human mesenchymal stem cells differentiate into keratocyte-like cells in keratocyte-conditioned medium. *Exp Eye Res* 101:16-26.
69. Hassell JR and DE Birk. (2010). The molecular basis of corneal transparency. *Exp Eye Res* 91:326-35.
70. Desai VD, HC Hsia and JE Schwarzbauer. (2014). Reversible modulation of myofibroblast differentiation in adipose-derived mesenchymal stem cells. *PLoS One* 9:e86865. doi:10.1371/journal.pone.0086865
71. Jester JV, WM Petroll, PA Barry and HD Cavanagh. (1995). Expression of alpha-smooth muscle (alpha-SM) actin during corneal stromal wound healing. *Invest Ophthalmol Vis Sci* 36:809-19.
72. Maycock NJ and J Marshall. (2014). Genomics of corneal wound healing: a review of the literature. *Acta Ophthalmol* 92:e170-84. <https://doi.org/10.1111/aos.12227>
73. Sekiya I, JT Vuoristo, BL Larson and DJ Prockop. (2002). In vitro cartilage formation by human adult stem cells from bone marrow stroma defines the sequence of cellular and molecular events during chondrogenesis. *Proc Natl Acad Sci USA* 99:4397-402.

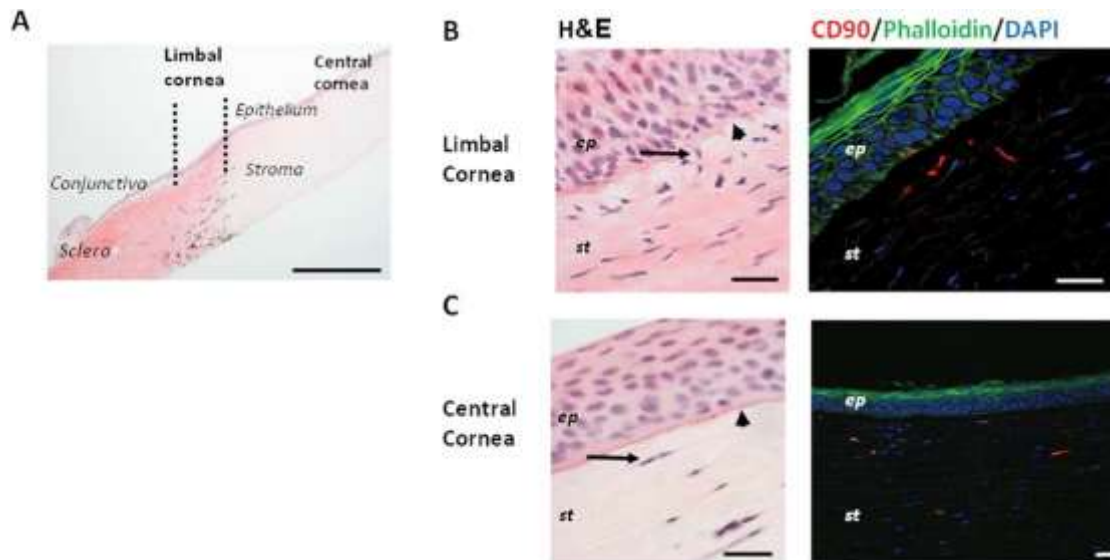


Figure 1 Histological and immunohistochemical staining of the canine limbal and central cornea with H&E and CD90. **(A)** an anatomical overview of the sclera, limbal (indicated by dashed lines) and central cornea (H&E stain); **(B)** the limbal cornea demonstrates an irregular, thickened and undulated basement membrane (arrow head, H&E) with close proximity of stromal cells (black arrow). **(C)** In the central cornea a fine regularly formed basement membrane is present (arrow head, H&E) and the keratocytes are more distant from the basement membrane (black arrow, H&E). **(B)** A distinct population of CD90 + expressing stromal cells were present in the limbal (CD90) and central anterior-mid stroma (CD90). Nuclei are shown by DAPI counter staining and the cytoskeleton by Phalloidin. Scale bars: 500 μ m (A) 20 μ m (B, C); Abbreviations: ep, epithelium; st, stroma.

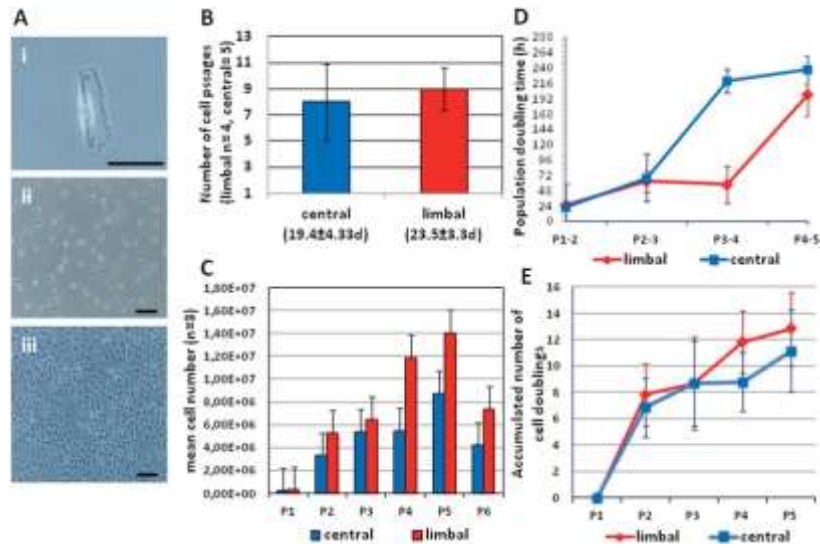


Figure 2 Cell morphology and culture kinetics of limbal versus central corneal stromal cells (CSC). **(Ai)** Phase contrast images demonstrate the adherent, small, ovoid morphology of CSC. **(Aii)** The cell morphology changes to a more elongated, stellate shape intermixed with small ovoid cells up to 60-70% confluency. **(Aiii)** With increasing confluency, a syncytium of stellate, elongated cells were formed. **(B)**: Maximal number (mean \pm SD) of cell passages in number of days (mean \pm SD) and **(C)** cell counts over 6 passages (mean \pm SD) showed no significant difference between limbal and central CSC. **(D)**: The population doubling time (h) and **(E)** cumulative number of cell doublings showed exponential growth over 5 passages and then reached senescence. There was no significant difference between central and limbal CSCs. Scale bar: 20 μ m; Abbreviations: h, hours; n, number of biological replicates; P, passages.

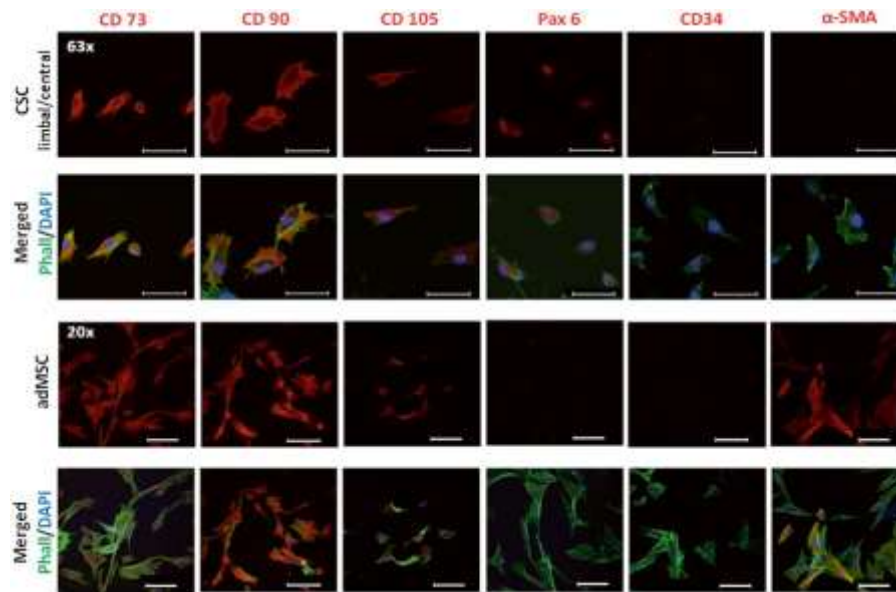


Figure 3 Immunocytochemical profile of CSC in comparison to canine adipose derived mesenchymal stromal cells (adMSC): CSC and adMSC expressed CD73, CD90, CD105 but not CD34; only CSC expressed Pax6 and only adMSC expressed α -SMA. Limbal and central CSCs showed the same staining profile. Nuclei are shown by DAPI counter staining and the cytoskeleton by Phalloidin (Phall). Scale bar: 20 μ m; magnification: CSC (63x), adMSC (20x)

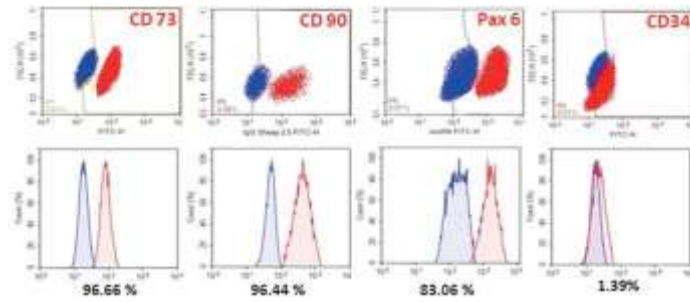


Figure 4 Quantification of MSC markers and Pax6 in limbal CSCs by flow cytometry. Cell quantification demonstrated in dot plots (FITC-H/FSC-H) and histograms of normalized cell counts (%) of positive gated limbal CSC (red) with an overlap allowance of 2% to the IgG isotype (blue). 96.66% of limbal CSC were CD73+, 96.44% CD90+, 83.06% Pax+ and 1.39% CD34+. (% in mean, n=3). Abbreviations: FSC-H, forward scatter height; FITC-H, Fluorescein isothiocyanate height; n, number of biological replicates.

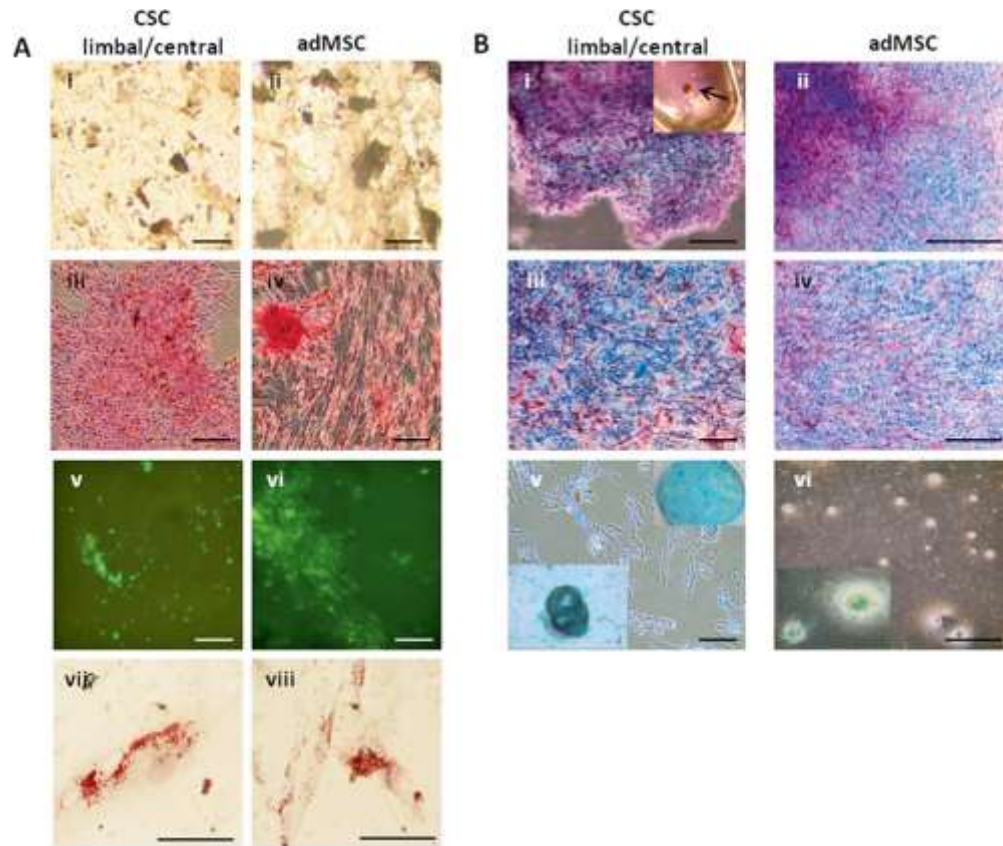


Figure 5 Trilineage differentiation of limbal/central CSC, adMSC **(A)**: Osteogenic differentiation of CSC (A i, iii, v) and adMSC (A ii, iv, vi) was confirmed via von Kossa (A i, ii), Alizarin S red (A iii, iv) and inorganic hydroxyapatite stain (Lonza®) (A v, vi) . Adipocyte differentiation of CSC (A vii) and adMSC (A viii) was confirmed with oil red O stain. **(B)**: Chondrogenic differentiation of CSC (B i) in pellet form (see black arrow, photography of falcon tube inserted) and adMSC (B ii) and in higher magnification (B iii, iv) showed blue stained glycosaminoglycans deposits using Alcian blue stain between red counterstained stained cells. CSCs (B vi) and adMSC (B vii) showed chondrogenic differentiation in 2D (cell culture dish photography inserted) forming Alcian blue stained nodular formation (highlighted in magnified image boxes). There was no difference between limbal and central CSCs. Scale bar: 20 μ m, B i,ii: 500 μ m

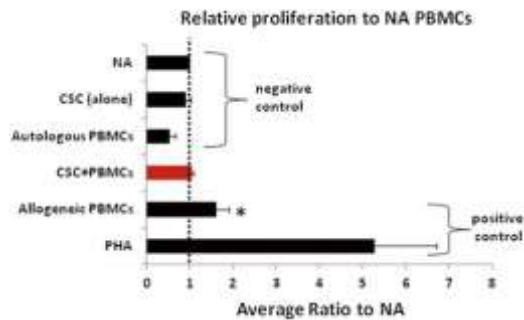


Figure 6 The PBMC co-culture assay showed that allogeneic limbal CSC co-cultured with PBMCs (red bar) did not modify the baseline level of non-activated PBMC proliferation (NA). In comparison co-cultures of effector PBMCs with allogeneic PBMCs showed a significant increase in proliferation compared to non-activated PBMC ($P < 0.01$). The values represent the mean average proliferation ratio (\pm SE) to non-activated PBMC highlighted with a dashed line; $n=3$, *, $p < 0.05$. Abbreviations: CSC, corneal stromal cells; NA, non-activated; PBMC, peripheral blood mononuclear cells; PHA, Phytohemagglutinin; n, number of biological replicates.

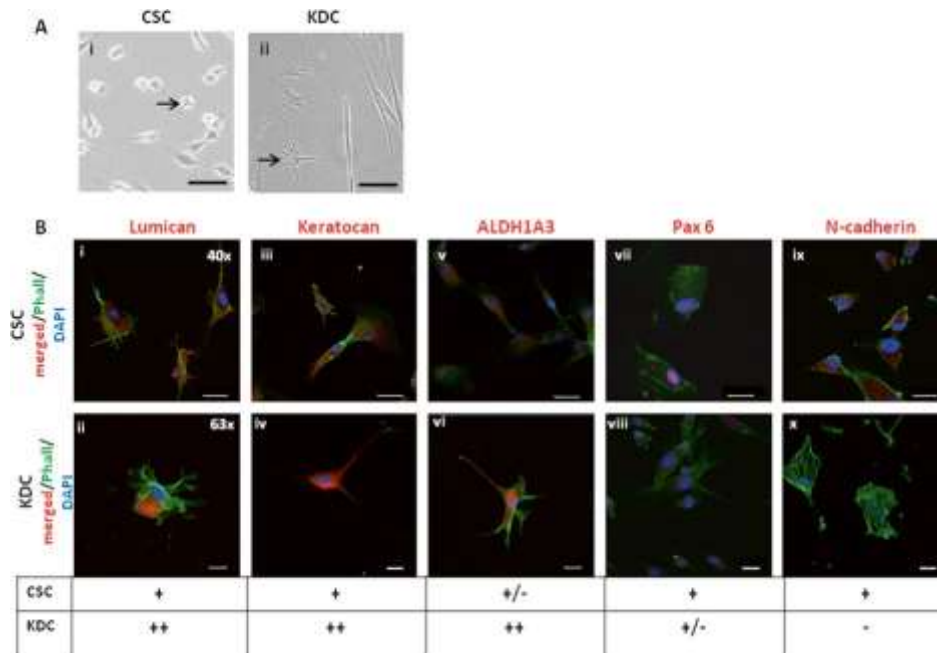


Figure 7 Limbal corneal stromal cells (CSC) differentiation into keratocyte-like cells (KDC) *in vitro*. **(A)**: Phase contrast images of CSC **(Ai)** demonstrated the increased cell size, stellate and elongated cell morphology of KDC **(Aii)** highlighted by the black arrows. **(B)**: Images and table summarized the immunocytochemistry staining results. Keratocyte markers Lumican, Keratocan and ALDH1A3 in KDC were more strongly expressed than in CSC, the nuclear stem cell marker Pax6 was weaker and N-cadherin was not expressed. Nuclei are shown by DAPI counter staining and the cytoskeleton by Phalloidin (Phall). Scale bar: 20 μ m; magnification: CSC (40x), KDC (63x).

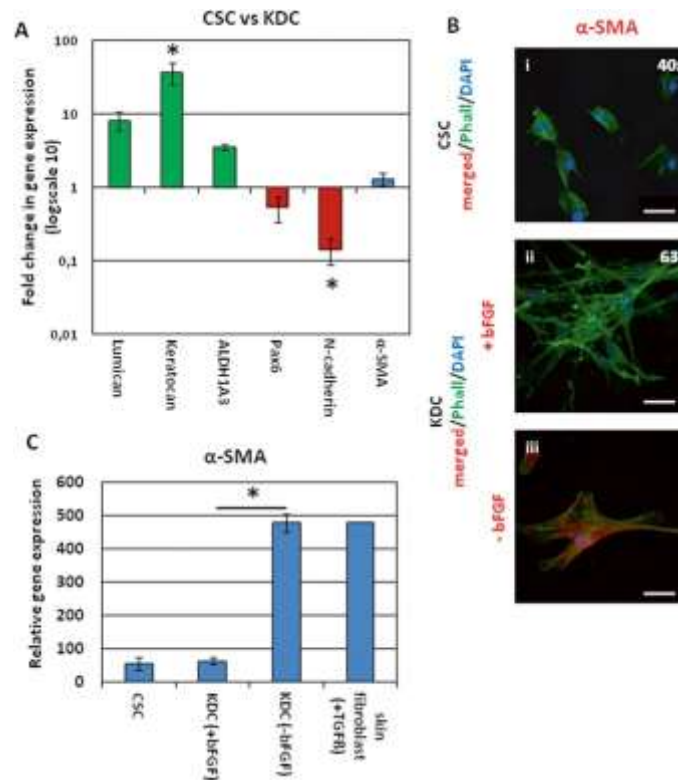


Figure 8 Limbal corneal stromal cells (CSC) differentiation into keratocyte-like cells (KDC) *in vitro*. **(A)**: Fold changes of quantitative reverse transcriptase polymerase chain reaction expression data showed the upregulation of *Lumican*, *Keratocan* ($P < 0.05$), *ALDH1A3* and down regulation of *Pax6*, *N-cadherin* ($P < 0.001$). *A-SMA* was up regulated. Values represent mean \pm SE, $n=3$,*, $p < 0.05$. Abbreviations: n, number of biological replicates. **(B)**: Immunocytochemical marker expression of α -SMA (red) of CSC versus KDC. KDC cultured with bFGF did not express α -SMA but in the absence of bFGF ($-$ bFGF) α -SMA was expressed. Nuclei are shown by DAPI counter staining and the cytoskeleton by Phalloidin (Phall). Scale bar: $20\mu\text{m}$; magnification: CSC (40x), KDC (63x). **(C)**: Quantitative reverse transcriptase polymerase chain reaction relative gene expression data of α -SMA in KDC cultured without ($-$ bFGF) showed significant ($P < 0.001$) upregulation compared to CSC and KDC cultured with bFGF (+bFGF). Skin fibroblast cultured with substituted TGF β to induce up regulation of α -SMA served as positive control. Values represent mean \pm SE, $n=3$,*, $p < 0.05$. Abbreviations: bFGF, basic human fibroblast growth factor; TGF β , transforming growth factor beta.

Supplementary Table S1. Donor details				
Case#	Age (years)	Sex	Breed	Tissue
1	1.3	m	Staffordshire bull terrier	Cornea Os/Od
2	1.2	m	Staffordshire bull terrier	Cornea Os/Od
3	1.5	m	Staffordshire bull terrier	Cornea Os/Od
4	1.8	m	Staffordshire bull terrier	Cornea Os/Od
5	2	fs	Cross breed	Cornea Os/Od
6	1	m	Staffordshire bull-cross breed	Cornea Os/Od
7	6 weeks	m	Dalmatian	Cornea Os
8	6weeks	m	Dalmatian	Cornea Od
9	8weeks	f	Old english sheepdog	Cornea Os/Od
10	8	mn	Springer spaniel	Cornea Os/Od
11	12	mn	Lurcher	Cornea Os/Od
12	12	mn	Golden retriever	Cornea Os/Od
13	2	fs	Border collie	Cornea Os/Od
14	8	fs	Labrador	Cornea Os/Od
15	11	mn	Mix	Subcutaneous fat (adMSC)
16	8	mn	Irish setter	Subcutaneous fat (adMSC)
17	6 weeks	m	Dalmatian	Subcutaneous fat (adMSC)
18	8weeks	f	Bull terrier	Popliteii lymph nodes

19	4.8	fs	Pug	Popliteii lymph nodes
20	6	f	Cross-breed	PBMC (3H biomedical)
21	6	m	Labrador retriever	PBMC (3H Biomedical)

The table summarizes the donor details of dogs including age (years/weeks), sex, breed and tissue donated. Abbreviations: adMSC, adipose derived mesenchymal stromal cell; PBMC, peripheral blood mononuclear cells; f, female; fs, female- spayed; m, male; mn, male-neutered; od, ocular dexter; os, ocular sinister

Supplementary Table S2: Antibodies used for Immunofluorescence Staining (IF), Western Blotting (WB) and Flow Cytometry (FC)			
Antibodies	Sources	Dilution	MW (kDa)/band size (WB)
Anti-Pax 6	Biolegend (901301, Clone: Poly 19013, San Diego, CA, USA)	1:500 for IF 1:100 for WB 2 μ g/10 ⁶ cells for FC	47-50
Alpha-SMA	Abcam (ab5694, Cambridge, UK)	1:200	42 [1]
ALDH1A3	Abcam (ab129815, Cambridge, UK)	1:500 for IF 1:500 for WB	56 (unspecific bands 30 and 15)
CD34	Abcam (ab81289, Cambridge, UK)	1: 100 for IF 1:1000 for WB 2 μ g/10 ⁶ cells for FC	120
CD73	Bioss (bs-4834R, Woburn, MA, USA)	1:300 for IF 1:500 for WB 2 μ g/10 ⁶ cells for FC	Isoform 1: 63 Isoform 2: 58
CD90	R&D systems (AF 2067, Minneapolis, MN)	1:100 for IF 1:500 for WB	23-30

		2.5µg/10 ⁶ cells for FC	
CD105	Abcam (ab156756, Cambridge, UK)	1:200	70 [2]
Lumican	Abcam (ab168348, Cambridge,UK)	1:200 for IF 1:1000 for WB	36 (unsp.band 51kDa)
N-cadherin	Abcam (ab18203, Cambridge, UK)	1:100 for IF 1:1000 for WB	125-135
Keratocan	Biorbyt (orb2975, Cambridge,UK)	1:100 for IF 1:250 for WB	50 (unsp. band 141, 41, 25kDa)
Secondary and control antibody			
Anti Sheep IgG HRP	R&D systems (HAF016, Minneapolis, MN)	1:1000 for WB	
Anti-Sheep IgG-NL557	R&D systems (NI 010, Minneapolis, MN)	1:200 for IF	
Anti-Sheep IgG- NL493	R&D systems (NI 012, Minneapolis, MN)	1:200 for FC	
Anti-Rabbit IgG HRP	Dako (Agilent Technologies, Santa Clara, CA, USA)	1:1000 for WB	

Anti-Rabbit FITC	Sigma (F1262, Gillingham,UK)	1:100 for FC	
Alexa Fluor 594 goat anti-rabbit	Invitrogen (A-11037 Thermo Fisher, Paisley, UK)	1:500 for IF	
Alexa Fluor 594 goat anti-mouse	Invitrogen (A-11032Thermo Fisher, Paisley, UK)	1:500 for IF	
β -actin loading control	Section 1.01 Abcam (ab20272, Cambridge, UK)	1: 5000 for WB	42
Rabbit IgG (Control antibody)	Abcam (ab27478, Cambridge, UK)	1:500 for IF	
Mouse IgG2a (Control antibody)	Biologend (401501,Clone: MG2a-83, San Diego, CA, USA)	1:500 for IF	
Sheep IgG (Control antibody)	R&D systems (5-001-A), Minneapolis, MN, USA)	1:200 for IF 2.5 μ g/10 ⁶ cells	

		for FC	
Rabbit IgG (Control antibody)	Section 1.02 Vectashield laboratories (I-1000-5, Peterborough, UK	2µg/10 ⁶ cells for FC	

The table summarizes the antibodies used for Immunofluorescence Staining (IF), Western Blotting (WB), Flow Cytometry (FC) and information of the company details, catalogue number, dilution and molecular weight (MW) in kDA (kilo Dalton)/ band size.

Reference

1. Mai J, Q Hu, Y Xie, S Su, Q Qiu, W Yuan, Y Yang, E Song, Y Chen and J Wang. (2015). Dysynchronous pacing triggers endothelial-mesenchymal transition through heterogeneity of mechanical stretch in a canine model. *Circ J* 79:201-9.
2. Hensley MT, J Tang, K Woodruff, T Defrancesco, S Tou, CM Williams, M Breen, K Meurs, B Keene and K Cheng. (2017). Intracoronary allogeneic cardiosphere-derived stem cells are safe for use in dogs with dilated cardiomyopathy. *J Cell Mol Med* 21:1503-1512.

Supplementary Table S3. Primer Sequence Used for Real-time PCR			
Gene Name	Forward	Reverse	Product size (bp)
Lumican	AAACATTTGCGTCTGGATGG	TATCAGGTGGCAGACTGGTG	55
Keratocan	TCATCTGCAGCACCTTCATC	TGATTCATTGCCATCCAGA	146
ALDH1A3	GCCCTTTATCTGGGCTCTCT	GACCCCGTGAAGGCTATCTT	137
N-cadherin	TGTGAACGGGCAAATAACAA	AGATCTGCAGCGTTCCTGTT	137
Pax6	ATTACTGTCCGAGGGGGTCT	CTAGCCAGGTTGCGAAGAAC	81
Alpha-SMA	ACTGGGACGACATGGAAAAG	CACGGAGCTCGTTGTAGAAA	54
Canine 18S	CCGCAGCTAGGAATAATGGA	CCTCAGTTCGAAAACCAAC	61

The table summarizes the forward and reverse primer sequence used for real-time PCR and the product size in base pair (bp).